

## MONITORING OF FLUIDIC MUSCLES BY INFRARED THERMOGRAPHY

Enrico Ravina

Dept. of Mechanics and Machine Design – University of Genoa, Via Opera Pia 15A, 15145 Genoa, Italy  
enrico.ravina@unige.it

---

### Abstract

The paper discusses an approach to monitoring fluidic muscles, applying a non invasive thermal analysis based on infrared thermography. Different working dynamic conditions strongly modify the internal distribution of temperature of muscles, and the thermal gradients can be used as monitoring variables in order to check the correct behaviour of this type of component. A wide research activity, oriented to investigate on correlations between muscle performances and temperature distribution, is under development. This paper collects the result of the first phase of this activity, concerning experimental evaluations of thermal distribution and their relation to specific physical variables.

**Keywords:** pneumatics, muscles, monitoring, thermography

---

### 1 Introduction

Fluidic muscles are innovative pneumatic components able to mimic human muscular movements through contraction and extension phases. Practically they are tensile actuators formed by a pressure-tight rubber hose with terminal press-fitted or screwed metallic connections. The rubber hose is sheathed in high-strength fibres, creating a rhomboidal three-dimensional pattern. A compressed air flow inwards change the shape of the three-dimensional grid structure, generating a force along its neutral axis. The internal pressure increases and that causes a shorten up of the muscle, realizing, at most, a stroke of a quarter of its initial unloaded length. The first architecture of muscle modeling has been proposed by McKibben in the 1950s, in order to motorize pneumatic arms to help control handicapped hands. Its structure was very simple, with a rubber inner tube, closed by two ends, covered with a shell braided according to helical weaving. Starting from this initial idea several studies and improvements have been implemented concerning modelling, simulation, control techniques, materials and practical applications. Today one of the most interesting and reliable solutions consists on a multi-layered structure in which a gas-tight rubber liner is permanently joined to independently spiralled aramid fibre layers. Together they form a desired diamond pattern. The rubber sheath is poly-chloroprene, a rubber having a desired gas impermeability, very flexible, resistant and providing excellent adhesion to the textile fibres.

The main features of this type of actuators concern the initial force (up to 10 times higher than a conventional pneumatic actuator of the same diameter), a good dynamic response (also in presence of high loads), any mechanical parts in relative motion (zero leakage), simple control technology both for high frequency and extremely low movements. The device is very versatile and able to be used in a wide spectrum of applications. Very significant and extreme dynamic responses can be reached: frequencies up to 100 Hz (of course depending on the working stroke), velocities from 0.001 mm/s up to 3 m/s, accelerations up to 100 m/s<sup>2</sup>, forces up to 6000 N. Additional features of compactness and lightness allow the application of fluidic muscles in the place of traditional pneumatic actuators.

Images of different length fluidic muscles with screwed end connections and a sectioned view, showing the multi-layer body and the metallic terminal, are reported in Fig. 1.

However the optimal behaviour and the life cycle of this type of component is influenced by a wide spectrum of parameters, as:

- a supply of correctly prepared compressed air;
- the environmental conditions;
- the mechanical stresses during the initial mounting (torsional torques, transversal offset and angle between the connections,...);
- unbalancing of moved masses;

---

This manuscript was received on 7 November 2005 and was accepted after revision for publication on 17 July 2006

- input and output paths of the air flow inside the muscle;
- type and relative positions of air fittings.



Fig. 1: Fluidic muscles and sectioned view

In order to develop optimised designs involving pneumatic muscles in non conventional or advanced applications, a very deepened knowledge of actual characteristic and operating limits of these devices must be reached. Considering the particular nature of the components, the information available from catalogues of manufacturers are often not enough to a correct selection or, more in general, to evaluate the actual performances under specific working conditions.

Elements requiring additional information are, for instance:

- hysteresis cycles under different pressure load;
- repeatability errors on programmed motions;
- reproducibility;
- dynamic response to different excitation laws;
- relations between contraction and frequency;
- achievement of intermediate positions;
- inside temperature distribution.

Starting from these considerations a specific research activity oriented to correlate the mechanical performances of fluidic muscles to their thermal distribution has been initiated. In this paper, aspects on experimental testing of a non invasive monitoring method, based on infrared thermography technique, are presented and discussed.

## 2 Thermography as Monitoring Tool for Pneumatic Devices

Conventional pneumatic components are usually studied in isothermal conditions; this hypothesis may be often assumed because, excluding extreme applications, the temperature variations of the compressed air inside the pneumatic devices are limited and don't influence, in significant way, their dynamic response or their performance. It essentially depends on the mechanical structure of these components; cylinders or valves are made by rigid bodies, and thermal variations can locally influence only internal seals. This hypothesis, often applied in traditional pneumatic design, is not acceptable in presence of special components (slot-type

actuators, high frequency micro-valves,...) and, in particular, for tensile components, like muscles. The inside temperature distribution can drastically change as a function of the internal flow of the air, the position of pneumatic connections on the heads (lateral or axial), the working frequency, the pressure. In addition the composite structure of a muscle must be considered; the body in rubber and textile layers are interfaced to metallic terminations. The stress-strain behaviour is significantly different and particular criticalities can be generated within the junction cross sections between these parts. Local overheating or ununiform temperature distributions can be generated by particular working conditions or by the method used to supply and discharge the air within the muscle.

The variable geometry of a fluidic muscle, with continuous surface contraction and stretching, doesn't allow the measurement of the inside temperature and the surface temperature by means of traditional sensors (thermocouples). Infrared thermography seem to be a good monitoring tool, allowing non contact measurement while the equipment is online. The heat is produced within the muscle but it is not directly visible to the camera; it must conduct, through the composite layers of the muscle, and present itself as a pattern on the outside surface, in order for the infrared camera to sense it. Thermal imaging can be an effective method to monitor the thermal response of a muscle. Comparisons between standard and anomalous distributions enhance the ability to predict equipment troubleshooting or failure for the designer.

The periodic deformation of the muscle, with cyclic contraction and extension of fibres, is the main source of the heat and influences the temperature distribution inside the muscle. The observed temperature depends also on the input air flow, related to the working frequency. In order to split the detected temperature to different heat phenomena a next step of this study will analyse all possible connections between the muscle and pneumatic circuit. In particular, the case of input and output paths from opposite sides of the device ("washing" techniques) will be studied.

The basic theoretical reference for thermography is the Stefan-Boltzmann law for a "grey" body:

$$q = \epsilon \sigma_0 T^4 \quad (1)$$

where  $q$  is the emissive power ( $W/m^2$ ),  $\epsilon$  is the emissivity of the surface material,  $\sigma_0$  the Stefan-Boltzmann constant ( $5.67 \cdot 10^{-8} W/m^2 K^4$ ) and  $T$  is the absolute temperature of the surface body.

Considering a real case, materials present emissivities lower than unit. A radiometer positioned in front of a body detects both the emitted radiance and the radiance due to the reflection of the environment fluxes by the object surface. The general relationship correlating the effective radiance  $L$  to the surface temperature is:

$$L = \tau \epsilon L^0(T) + \tau (1 - \epsilon) L^0(T_a) + (1 - \tau) L^0(T_{atm}) \quad (2)$$

where  $L$  is the radiance ( $W/m^2 \text{srad}$ ),  $L^0$  the total radiance of the ideal blackbody,  $\tau$  the effective atmospheric transmissivity,  $T$  the temperature of the object (derived from the measurement of the radiance  $L$ ),  $T_{atm}$  the temperature of the nonscattering isothermal atmosphere

and  $T_a$  the temperature of isothermal surroundings.

An infrared sensor measures the thermal energy emitted by a body; then the evaluation of temperature  $T$  is possible if the radiance  $L$  of the body is known. The emissivity  $\epsilon$  depends on the material and wave length. Table 1 (proposed by Infrared Solutions, Inc. Plymouth, U.S.A.) shows, for instance, typical values of  $\epsilon$  for different kinds of rubber.

**Table 1:** Reference data for emissivity

Material	Wave length [ $\mu\text{m}$ ]	Temp. [ $^{\circ}\text{K}$ ]	Emissivity
Rubber	8-12	303	0.95
Hard rubber	2-5	303	0.95
Bright hard rubber	2-5	303	0.94
Elastic rubber	2-5	303	0.86
Rough rubber	2-5	303	0.86

Using infrared thermo-cameras the evaluation of the surface temperature is affected by an error depending on the shape of the emitting body; in the present study a pneumatic muscle can be considered as a body having a cylindrical symmetry.

The surface temperature shown by the camera must be corrected taking into account the shot angle  $\Phi$  between body and camera. In other words, the estimated temperature must be corrected because the temperature of a cylindrical body is evaluated on the flat measurement plane of the instrument. This aspect will be briefly discussed hereafter, analysing the results of the present study.

Finally, the correct selection of the ambient temperature must be considered. In the following analyses the ambient temperature is continuously monitored and acquired by a digital thermometer, in order to deduce information on the convection phenomena in the muscle surroundings.

### 3 The Experimental Set-up

In order to investigate on the correlation between mechanical behaviour of muscles and their internal distribution temperature an original workbench has been designed and realized (in co-operation with FESTO Italy).

Figure 2 reports an overall view of the instrumented set-up; it consists on a metallic frame where muscles having different size (for diameter and length) can be tested. An antagonist pneumatic cylinder is interfaced to the muscle, through a mobile plate, simulating the external load.

The system allows the user to modify the spatial position of the frame including the muscle, the vertical alignment between the end terminals and their relative angle (Fig. 3). In this way a muscle can be tested generating any kind of misalignments between the metallic terminals.

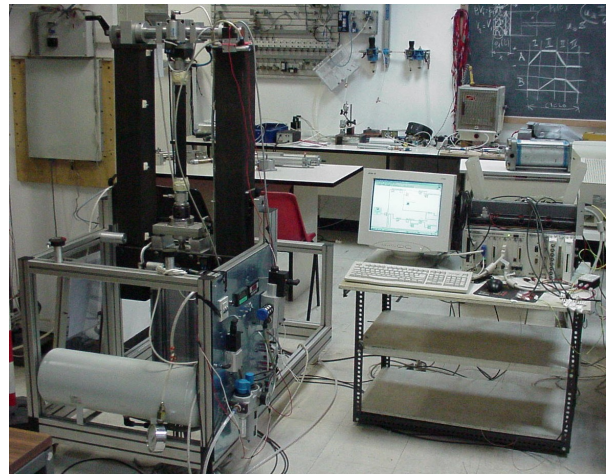


**Fig. 2:** The experimental set-up.

The workbench is instrumented with a load cell on the muscle (Fig. 4), pressure transducers on the muscle and on the antagonist actuator, linear displacement encoder and, externally, with an infrared thermo-camera equipped with a micro-lobometric VOx not cooled sensor. The accuracy of the infrared unit is  $0.1^{\circ}\text{C}$ , with excellent repeatability.

The camera is interfaced to the control unit in such a way the sequences of pictures can be synchronised to the selected motion laws, and in particular, to the dwell phases, optimising the image quality.

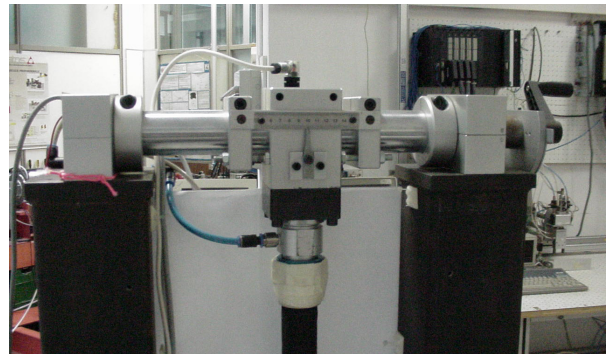


**Fig. 3:** Detail of the misalignment device.



**Fig. 4:** Detail of the antagonist cylinder and of the load cell.

Both cylinder and muscles are driven by on/off valves or by force control proportional valves (Fig. 5). On-off valves, switched by a timer, drive the muscle if standard sequences under variable frequencies are generated. In addition, all possible working conditions can be simulated, generating a programmed time history of input functions.



Fig. 5: Detail of pneumatic proportional valves.

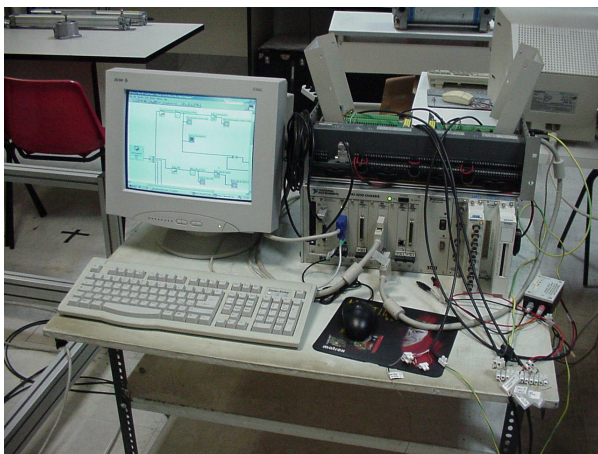


Fig. 6: Acquisition and elaboration unit.

All workbench functions are automatically managed by a flexible acquisition and elaboration unit, interfaced to the user through virtual instruments, originally implemented on PC (Fig. 6).

The camera elaborates the infrared radiance of any single point of the image (muscle surface), so as to evaluate the true temperature at that surface point. The main assumptions applied concern:

- neglect the infrared absorption of the air path between the muscle and the instrument;
- there is no infrared energy transmitted through the muscle from sources behind the same muscle.

In order to correct for reflection of the ambient instrument background, the inputs of the background temperature and the surface emissivity are required by the user. Details of procedure for measuring the effective emissivity of an unknown emitter are described in technical literature (Accetta and Shumaker, 1993; Fig. 7); in this particular application a specific algorithm to compensate the emission the cylindrical shape of the muscle has been implemented.

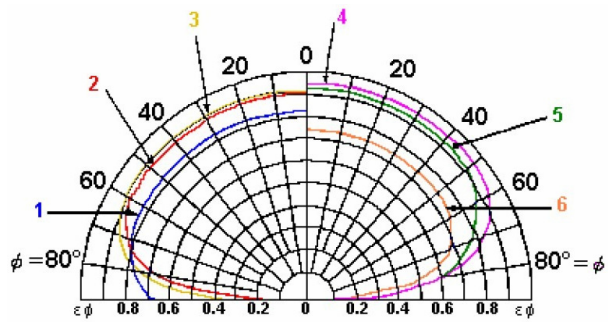


Fig. 7: Effect of the shot angle (1.  $Al_2O_3$ , 2. Paper, 3. Wood, 4. Ice, 5. Glass, 6.  $CuO_2$ ).

A compensation function relating the muscle emissivity to the shot angle  $\Phi$  between target and infrared camera has been evaluated and applied to the thermography results.

#### 4 Some Thermal Results

Metallic end connections have been shielded with special adhesive tape in order to eliminate reflectivity effects. The same technique has been applied on all metallic or reflecting surfaces (air, fittings, hoses, ...).

Tests have considered FESTO's fluidic muscles with screwed connections, equipped with a force-safety device in order to avoid force overloads.

The maximum contraction factor suggested by the manufacturer is 25 %. Three different muscle lengths have been tested in this study: 360, 240 and 120 mm (net length of the muscle, excluding terminations). Cycle frequencies, contraction amplitudes and internal pressures can be modified. Actual displacement of the muscle under programmed applied loads (by antagonist cylinder), forces, pressures and corresponding temperatures distribution are monitored. The aim is to research all possible correlations between muscle cinematic and dynamic performances and temperature distributions. In particular, correspondences between actual position errors and temperatures may be a significant monitoring reference of correct working conditions. Variations of these correlations could give information about possible anomalous conditions or about incoming failures.

Hereafter some significant results, concerning muscle with closed lower end terminal and upper lateral air connection (single acting component), are discussed.

The on/off experimental testing is organized on a single position or sequences of positions: the key parameters are the input pressure at the muscle, the input pressure at the antagonist cylinder, the contraction factor and the frequency. Repeatability tests are organized selecting the number of cycles for each programmed position. The selected default value is 500 cycles; a thermographical picture is automatically played every 10 cycles. Starting from the ambient temperature the muscle reaches its thermal steady-state condition after about 100 cycles. Experiments have considered the following ranges:

- frequency from 0.25 to 1 Hz;
- pressure from 1 to 6 bar;
- contraction factor from 10 to 25 %.

The proportional experimental tests are organized by programming the pressure laws on the muscle and on the antagonist actuator, in order to reach the programmed position with the best accuracy. These tests usually generate very slow contractions or stretching and, consequently, the muscle temperature remains practically constant.

#### 4.1 Effect of Length

Figure 8 reports the temperature map for a muscle of 360 mm length, 40 mm diameter, operating on 20 % of contraction, frequency of 0.25 Hz and pressure of 6 bar. We can notice that the warmest area is close to the lower terminal, with a vertical gradient of pressure of around 28 °C. The distribution is not perfectly symmetric, due to the lateral air connection.

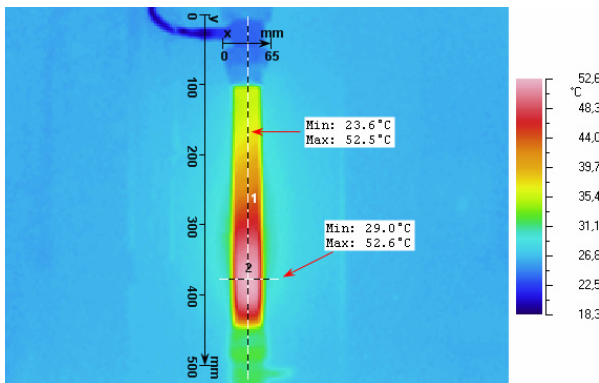


Fig. 8: Temperature map of a 360 mm muscle.

Figure 9 shows the vertical temperature profile; the upper terminal is cooled by the coming air. The temperature drop on the junction sections of the flexible cylinder with the metallic end terminations is significant.



Fig. 9: Temperature profile (360 mm muscle).

This temperature distribution is related to the air circuit, with input and output from the same side of the muscle. This choice is commonly used in industry, but it doesn't allow the "washing" of the muscle and only the fluid near to the upper terminal is able to mix with the inlet air. The fluid at the bottom is practically unfluenced to the air change.

A comparison with a short muscle (length of 120 mm) at the same working conditions is shown in Fig. 10; the temperature distribution is practically inverted, with the hot area close to the upper terminal which is, at the same time, the coolest element. It creates a very significant temperature gradient around the junction area. Figure 11 describes the corresponding temperature distribution; in this case the upper terminal is washed by the inlet air and its temperature decreases.

On the contrary, the flow rate is not enough to cool the muscle and that explains the "square" temperature function profile.

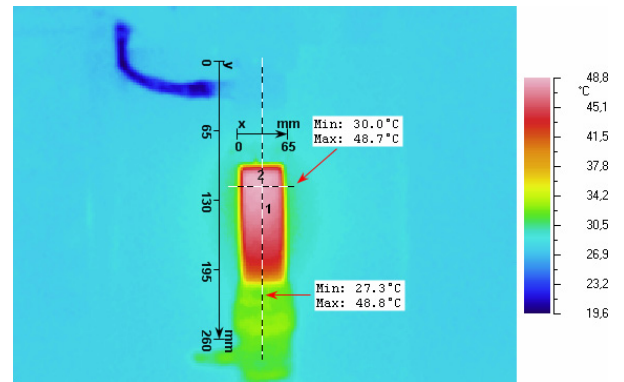


Fig. 10: Temperature map for a 120 mm muscle.



Fig. 11: Temperature profile (120 mm muscle).

#### 4.2 Effect of Frequency

Frequency excitation is another significant variable conditioning the behaviour of the muscle. Hereafter two different conditions for the same muscle (diameter 40 mm, length 360 mm), at the same air pressure (6 bar), are shown; in Fig. 12 the frequencies of the alternative motion applied to the muscle are, respectively, 0.25 and 1 Hz. Results are presented as density vs. temperature.

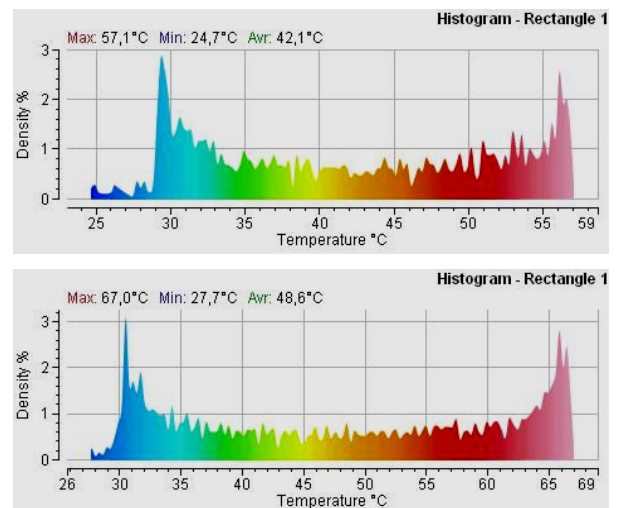


Fig. 12: Effect of frequency: a comparison.

The shape of the density distributions are similar, but the maximum temperature and the surface range of temperature increase with the frequency. In the second case the lower termination is colder than in the first one. Furthermore, a significant percentage of thermal

density is concentrated at high frequencies. Increasing frequency causes the maximum temperature increases, in according to the rules of heat exchange.

The influence of the frequency is related also on the length of the muscle; shorter muscles show a more uniform internal temperature distribution, with higher average values.

### 4.3 Effect of Pressure

The inlet air pressure modifies the thermal response on the muscle; that is particularly related to the relative position of the air fittings on the end terminations (axial or lateral, from on or two sides). Only one side lateral air supply (on the upper termination) is discussed in this paper. As previously cited, this is one of the most commonly applied techniques of connections, but it can be responsible of not optimised temperature distributions.

Figure 13 reports the corresponding results, respectively at 2 and 6 bar. Results are shown as temperature envelope profiles vs. pixels.

The muscle (diameter 40 mm, length 360 mm) is tested under a contraction factor of 20 %. The temperature distributions are similar only from a qualitative point of view; a more uniform temperature distribution is observed in the second case, with a higher average temperature.

The maximum temperature increases with pressure; this effect should be verified changing the size of the pneumatic valve, in order to make available different flow rates.

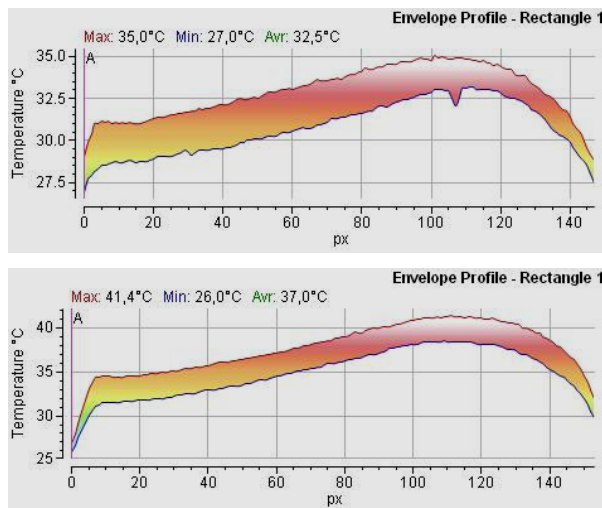


Fig 13: Effect of the inside pressure: a comparison.

## 5 Other Results

The test bench makes available other experimental information about the performance of the muscle. Particularly interesting are the force generated by the muscle vs. its contraction at different pressures (Fig. 14) and the position accuracy under repeated cycles, using on/off actuation (Fig. 15) or proportional actuation (for different contraction factors, Fig. 16).

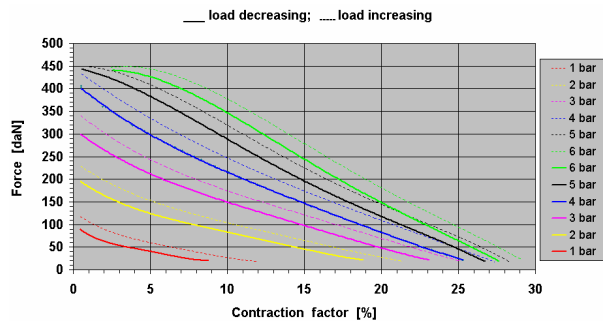


Fig 14: Force vs. contraction factor.

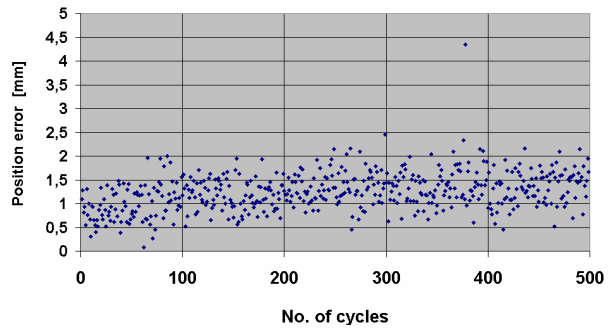


Fig 15: Accuracy (on/off actuation).

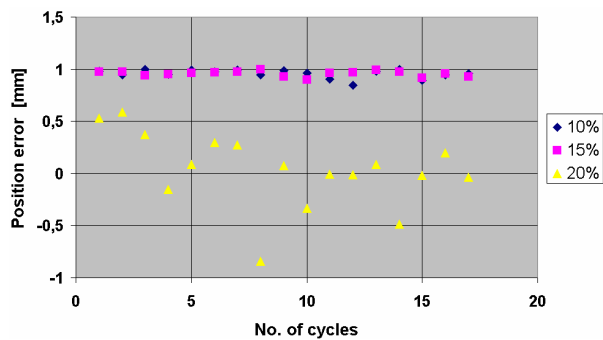


Fig 16: Accuracy (proportional actuation).

The activity is in progress; the next step is oriented to correlate these performance results to the thermal ones previously described, in order to collect full references about the behaviour of these pneumatic components. Resulting data will be used as a base of knowledge for monitoring under online testing.

## 6 Concluding Remarks

An approach of monitoring these pneumatic devices based on non intrusive temperature detection has been discussed. A methodical testing on three muscles having different length under very diversified working conditions has been developed. It makes now available a wide data base of mechanical and thermal information, still under elaboration. Presently, the theoretical and experimental activity is in progress and enhancement; next papers will discuss in detail other and more specific aspects, as correlations between position accuracy, frequency, length, pressure and temperature distribution. The synthesis of these experimental approaches will be the implementation of a theoretical model for monitoring and diagnostics.

## Nomenclature

$L$	radiance	[W/m <sup>2</sup> srad]
$L^0$	blackbody radiance	[W/m <sup>2</sup> srad]
$q$	emissive power	[W/m <sup>2</sup> ]
$T$	muscle temperature	[K]
$T_a$	temp. of isothermal surroundings	[K]
$T_{atm}$	atmospheric temperature	[K]
$\varepsilon$	effective muscle emissivity	
$\lambda$	wave length	[ $\mu$ m]
$\Phi$	shot angle	[degrees]
$\sigma_0$	Stefan-Boltzmann constant	[W/m <sup>2</sup> K <sup>4</sup> ]
$\tau$	effective atmospheric transmissivity	

## Acknowledgement

The experimental activity has been possible thanks to the support of FESTO Italy.

## References

- Accetta, J. S. and Shumaker, D. L.** 1993. *The infrared and electro-optical systems handbook*, (8 volumes), IIAC, Ann Arbor and SPIE Press, Bellingham, USA.
- Anon.** 2003. Muscling in on manufacturing. *Engineer*, Vol. 292, No. 7624, p. 40.
- Beomonte Zobel, P., Raparelli, T., Mattiazzo, G., Mauro, S. and Velardocchia, M.** 1998. Force control with fuzzy logic for pneumatic rubber muscles. *Proc. 29<sup>th</sup> Intl. Symposium on Robotics*, pp. 30-38.
- Bereichevsky, Y. and Lo, Y.** 2005. Fabrication of polypyrrole nanowires. *Proc. of SPIE*, Vol. 5729, pp. 268-273.
- Boblan, I., Bannasch, R., Schwenk, H., Prietzel, F., Miertsch, L. and Schulz, A.** 2004. A human-like robot hand and arm with fluidic muscles: Biologically inspired construction and functionality. *Lecture Notes in Artificial Intelligence*, pp. 160-179.
- Caldwell, D. G.** 1993. Natural and artificial muscle elements as robot actuators. *Mechatronics*, Vol.3, No. 3, pp. 269-283.
- Caldwell, D. G., Medrano-Cerda, G. A. and Goodwin, M.** 1995. Control of Pneumatic Muscle Actuators. *IEEE Control Systems*, Vol. 2, pp.40-48.
- Ferraresi, C., Franco, W. and Manuello Berretto, A.** 2001. Flexible pneumatic actuators: a comparison between the McKibben and the straight fibres muscles. *Journal of Robotics and Mechatronics*, Vol 13, No. 1, pp. 56-62.
- Ferraresi, C., Franco, W. and Manuello Berretto, A.** 1998. Modelisation and Charaterisation of a Pneumatic Muscle Actuator for Non Conventional Robotics. *Proc. 7th Intl. Workshop of Robotics in Alpe-Danube Region*, pp. 279-284.
- Hannaford, B., Jaax, K., and Klute, G.** 2001. Bio-Inspired Actuation and Sensing. *Autonomous Robots*, Kluwer Academic Publishers, Vol. 11, pp. 267-272.
- Infrared Solutions. 2004. *IR FlexCam<sup>®</sup> T User Manual*.
- Kimura, T., Hara, S., Fujita, T. and Kagawa, T.** 1997. Feedback linearization for pneumatic actuator systems with static friction. *Control Engineering Practice*, Vol. 5, No. 10, pp. 1385-1394.
- Klute, G. K. and Hannaford, B.** 1998. Fatigue Characteristics of McKibben Artificial Muscle Actuators. *Proc. IEEE/RSI Intl. Conf. On Intelligent Robots and Systems*, pp. 1776-1781.
- Maldague, X. P. and Moore, P. O.** 2001. *Non destructive thermal testing handbook, Vol.3, Infrared and thermal testing*, ASNT, Washington, USA.
- Mattiazzo, G., Mauro, S. and Velardocchia, M.** 1997. Design of pneumatic positioner with PID and fuzzy control. *Proc. 6<sup>th</sup> Intl. Workshop on Robotics in Alpe-Danube Region*, pp 429-434.
- Nortisugu, T. and Tanaka, T.** 1997. Application of Rubber Artificial Muscle as a Rehabilitation Robot. *IEEE/ASME Transactions on Mechatronics*, Vol.2, No.4, pp. 259-267.
- Quinn, R. D., Nelson, G. M. and Bachmann, R. J.** 2001. Toward Mission Capable Legged Robots through Biological Inspiration. *Autonomous Robots*, Kluwer Academic Publishers, Vol. 11, pp. 215-220.
- Raparelli, T., Beomonte Zobel, P. and Durante, F.** 2000. On the design of Pneumatic muscle actuators. *Internationales Fluidtechnisches Kolloquium*, Dresden, Germany.
- Sanchez, A., Mahout, V. and Tondu, B.** 1988. Nonlinear parametric identification of a McKibben artificial pneumatic muscle using flatness property of the system. *Proc. 1988 IEEE Intl. Conference on Control Application*, Trieste, Italy, pp. 70-74.
- Tanaka, Y.** Study of artificial rubber muscle. *Mechatronics*, Vol.3, No. 1, pp. 59-75.
- Tondu, B. and Lopez, P.** 2000. McKibben artificial muscle robot actuators. *IEEE Control Systems Magazine*, April 200, pp. 15-38.
- Tsagarakis, N. and Caldwell, D. G.** 2000. Improved Modelling and assessment of pneumatic Muscle Actuators. *Proc. Of the 2000 IEEE Intl. Conference on Robotics & Automation*, S.Francisco, CA, pp.3641-3646.
- Tuijthof, G. J. M. and Herder, J. L.** 2000. Design, actuation and control of an anthropomorphic robot arm. *Mechanism and Machine Theory*, Vol. 35, pp. 945-962.

**Van de Linde, R. Q.** 1999. Design, Analysis, and Control of a Low Power Joint for Walking robot, by Phasic Activation of McKibben Muscles. *IEEE Transactions on Robotics and Automation*, Vol. 15, No.4, pp 599-604.

Additional references concern internet web sites:

[www.festo.com](http://www.festo.com);

[www.shadow.org.uk](http://www.shadow.org.uk);

[www.improtec.it](http://www.improtec.it);

[www.mediarelations.lanxsess.com](http://www.mediarelations.lanxsess.com) and others in the fields of the innovative pneumatics and the thermography.



**Enrico Ravina**

Associate professor at the Dept. of Mechanics and machine design of the University of Genoa (Italy). He teaches Fluid Power Automation and Mechanics of Machinery. His current research interest regard pneumatics, oil-hydraulics and their development in mechatronic fields. Authors of about 200 publications, he has been member of many international scientific committees, reviewer for international journals, UNI and ISO expert.